JGR Atmospheres

RESEARCH ARTICLE
10.1029/2021JD034826

Key Points:

- Heterogeneous reactivity of $CaCO_3$ toward NO_2 was limited at <1% relative humidity (RH), with uptake coefficient estimated to be $<2 \times 10^{-8}$
- This reaction was enhanced at elevated RH, and average uptake coefficients were measured to be $\sim 1.2 \times 10^{-7}$ at 20%–80% RH
- Heterogeneous reaction with NO_2 significantly increased hygroscopicity of $CaCO_3$ particles

Supporting Information:

Supporting Information may be found in the online version of this article.

Correspondence to:

M. Tang,
mingjintang@gig.ac.cn

Citation:

Jia, X., Gu, W., Peng, C., Li, R., Chen, L., Wang, H., et al. (2021). Heterogeneous reaction of $CaCO_3$ with NO_2 at different relative humidities: Kinetics, mechanisms, and impacts on aerosol hygroscopicity. *Journal of Geophysical Research: Atmospheres*, *126*, e2021JD034826. https://doi.org/10.1029/2021JD034826

Received 2 MAR 2021
Accepted 18 MAY 2021

Author Contributions:

Conceptualization: Mingjin Tang
Investigation: Xiaohong Jia, Wenjun Gu, Chao Peng, Rui Li, Lanxiadi Chen
Resources: Hongli Wang, Haichao Wang, Xinming Wang, Mingjin Tang
Supervision: Mingjin Tang
Writing – original draft: Xiaohong Jia, Chao Peng, Lanxiadi Chen, Mingjin Tang
Writing – review & editing: Mingjin Tang

Heterogeneous Reaction of $CaCO_3$ With NO_2 at Different Relative Humidities: Kinetics, Mechanisms, and Impacts on Aerosol Hygroscopicity

Xiaohong Jia[1,2,3], Wenjun Gu[1,2,3], Chao Peng[1,2], Rui Li[1,2,3], Lanxiadi Chen[1,2,3], Hongli Wang[4], Haichao Wang[5], Xinming Wang[1,2,3], and Mingjin Tang[1,2,3]

[1]State Key Laboratory of Organic Geochemistry, Guangdong Key Laboratory of Environmental Protection and Resources Utilization, Guangdong-Hong Kong-Macao Joint Laboratory for Environmental Pollution and Control, Guangzhou Institute of Geochemistry, Chinese Academy of Sciences, Guangzhou, China, [2]CAS Center for Excellence in Deep Earth Science, Guangzhou, China, [3]University of Chinese Academy of Sciences, Beijing, China, [4]State Environmental Protection Key Laboratory of Formation and Prevention of Urban Air Pollution Complex, Shanghai Academy of Environmental Sciences, Shanghai, China, [5]School of Atmospheric Sciences, Sun Yat-sen University, Guangzhou, China

Abstract Heterogeneous reaction of NO_2 with $CaCO_3$, an abundant and reactive component in mineral dust aerosol, was investigated in this work at different relative humidifies (RH, up to 80%), using a fixed-bed reactor. Ion chromatograph and a vapor sorption analyzer were employed to measure changes in particulate nitrate and water with reaction time (up to 24 h). When NO_2 concentration was ~10 ppmv ($\sim 2.5 \times 10^{14}$ molecule cm^{-3}), $CaCO_3$ showed very low reactivity toward NO_2 at <1% RH, and $\gamma(NO_2)$ was estimated to be $<2 \times 10^{-8}$; consequently, no significant change in hygroscopicity of $CaCO_3$ particles was observed after reaction with NO_2 for 24 h at <1% RH, as the amount of nitrate formed was very limited. Heterogeneous reactivity was significantly enhanced at elevated RH (20%–80%), and during the reaction $CaCO_3$ was covered with a deliquesced layer resulting from water uptake by formed nitrate; in addition, the average $\gamma(NO_2)$ was determined to be $(1.21 \pm 0.45) \times 10^{-7}$, independent of RH (20%–80%) and reaction time (3–24 h). After reaction with 10 ppmv NO_2 for 24 h at elevated RH (20%–80%), the mass of particulate water associated with reacted $CaCO_3$ at 90% RH was equal to ~45% of the mass of unreacted $CaCO_3$, suggesting that heterogeneous reaction of $CaCO_3$ with NO_2 at 20%–80% RH could substantially increase its hygroscopicity. Overall, our laboratory study suggested that heterogeneous reaction with NO_2 may significantly impact composition and hygroscopicity of $CaCO_3$ particles.

1. Introduction

Mineral dust is an important component of tropospheric aerosols (Ginoux et al., 2012; Textor et al., 2006), and can be transported over thousands of kilometers in the troposphere after being lifted from arid and semi-arid regions (Prospero & Mayol-Bracero, 2013; Uno et al., 2009). During transport, mineral dust particles may undergo heterogeneous and multiphase reactions with trace gases (Crowley et al., 2010; M. J. Tang et al., 2017; Usher et al., 2003), such as nitrogen oxides (NO_x). Heterogeneous reaction of mineral dust with NO_2, an important nitrogen oxide in the troposphere, may contribute significantly to the formation of aerosol nitrate and HONO (an important precursor of OH radicals) (Kumar et al., 2014; J. Li et al., 2012; Ndour et al., 2008; Y. Tang et al., 2004), and could thus affect the formation of O_3 (Dentener et al., 1996; Kumar et al., 2014; J. Li et al., 2012; Ndour et al., 2008; Y. Tang et al., 2004) and secondary aerosols (Dentener et al., 1996; Kumar et al., 2014; J. Li et al., 2012; Y. Tang et al., 2004). As a result, this reaction is of great interest and has been examined by a number of laboratory studies (Angelini et al., 2007; Borensen et al., 2000; El Zein & Bedjanian, 2012; H. J. Li et al., 2010; R. Li et al., 2020; C. Liu et al., 2017; Y. Liu et al., 2015; Ndour et al., 2008; Tan et al., 2016; Underwood et al., 1999; Zhang et al., 2012; Zhou et al., 2015).

Mineral dust is very complex and contains a variety of minerals (Journet et al., 2014; Nickovic et al., 2012; Scanza et al., 2015; M. J. Tang et al., 2016), among which calcite ($CaCO_3$) is abundant and reactive (Usher et al., 2003). To our knowledge, only two previous studies (H. J. Li et al., 2010; Tan et al., 2016) measured uptake coefficients of NO_2, $\gamma(NO_2)$, onto $CaCO_3$ particles, and both studies used diffuse reflectance infrared Fourier transform spectroscopy (DRIFTS) and ion chromatography (IC) to quantify nitrate formation due to

heterogeneous reaction with NO_2. The initial $\gamma(NO_2)$ were measured to be $(4.25 \pm 1.18) \times 10^{-9}$ when relative humidity (RH) was <10% and slightly decreased to $(2.54 \pm 0.13) \times 10^{-9}$ at 60%–71% RH (H. J. Li et al., 2010). A later study (Tan et al., 2016) found that increase in RH from <1% to 40% would reduce initial $\gamma(NO_2)$ from $(3.34 \pm 0.14) \times 10^{-9}$ to $(2.04 \pm 0.07) \times 10^{-9}$, while further increase in RH to 80% did not lead to significant change in $\gamma(NO_2)$. In both studies (H. J. Li et al., 2010; Tan et al., 2016), multiple layers of $CaCO_3$ particles, placed in sample holders, were exposed to NO_2, and $\gamma(NO_2)$ were calculated assuming that surfaces of all the particles were available for NO_2 uptake; however, this assumption may not be valid. Therefore, surface areas available for heterogeneous uptake may have been overestimated and uptake coefficients underestimated by a few orders of magnitude, as well documented in previous work (Crowley et al., 2010; M. J. Tang et al., 2017; Underwood et al., 2000).

The hygroscopicity of unreacted $CaCO_3$ is very low (Chen et al., 2020; Gustafsson et al., 2005; Ma et al., 2012; Sullivan et al., 2009a). Heterogeneous reactions of $CaCO_3$ with acidic trace gases produce more soluble and hygroscopic specie (for example, $Ca(NO_3)_2$) (Gibson et al., 2006; Guo et al., 2019; Sullivan et al., 2009a; M. J. Tang et al., 2016). This is supported by a number of field studies (Laskin et al., 2005; W. J. Li & Shao, 2009; Matsuki et al., 2005; Pan et al., 2019; Shi et al., 2008; Tobo et al., 2010) which found that some Ca-containing dust particles in the troposphere may exist as aqueous droplets, instead of solid particles as they were when freshly emitted. Laboratory work also showed that heterogeneous reactions with acidic trace gases could significantly enhance hygroscopicity of $CaCO_3$ (Al-Abadleh et al., 2003; Hatch et al., 2008; Krueger et al., 2003; Y. J. Liu et al., 2008; Ma et al., 2012; Sullivan et al., 2009b; Wang et al., 2018) and authentic mineral dust particles (Sullivan et al., 2010; Vlasenko et al., 2006). For example, after heterogeneous reaction with gaseous HNO_3 at 41% RH, solid $CaCO_3$ particles were transformed to deliquesced droplets (Krueger et al., 2003), due to the formation of highly hygroscopic $Ca(NO_3)_2$. In addition, it was found that HNO_3-reacted $CaCO_3$ could take up significant amount of water even at very low RH (~9%) (Al-Abadleh et al., 2003). Only one previous study (Y. J. Liu et al., 2008) explored the impacts of heterogeneous reaction of NO_2 on hygroscopic properties of $CaCO_3$, using micro-Raman spectroscopy coupled to a reaction cell in which RH could be well controlled. They found that after reaction with 100 ppmv ($\sim 2.5 \times 10^{15}$ molecule cm^{-3}) NO_2 at 37% RH for 50 min, $CaCO_3$ particles were converted to $CaCO_3/Ca(NO_3)_2$ particles which displayed much higher hygroscopicity and became deliquesced at ~10% RH; however, the amount of particulate water associated with reacted $CaCO_3$ particles was not quantified. The very limited laboratory work precludes us assessing to which extent heterogeneous reaction with NO_2 can increase hygroscopicity of $CaCO_3$ in the troposphere.

To better understand the impacts on nitrate formation and aerosol hygroscopicity, we employed a fixed-bed reactor to investigate heterogeneous reaction of $CaCO_3$ particles with NO_2 as a function of RH (0%–80%). The change in particle composition was measured offline using ion chromatography. NO_2 concentrations used in previous studies (H. J. Li et al., 2010; Y. J. Liu et al., 2008; Tan et al., 2016) were around or above $\sim 2.5 \times 10^{15}$ molecule cm^{-3}, at least one order of magnitude higher than those used in our work; therefore, compared to previous studies, NO_2 concentrations used in our work are closer to typical ambient levels. In addition, water uptake of unreacted and reacted $CaCO_3$ particles were measured offline using a vapor sorption analyzer, to determine the change in particle hygroscopicity. In our work laboratory, experiments were designed in a way so that we could monitor changes in both composition and particulate water of $CaCO_3$ during heterogeneous reaction with NO_2 under different conditions.

2. Methodology

2.1. Heterogeneous Reaction With NO_2

2.1.1. Preparation of $CaCO_3$ Particles

$CaCO_3$ (>99.5% Alfa Aesar) particles used in our work have a BET surface area of 2.18 ± 0.01 m^2/g and an average diameter of 3.12 ± 0.56 μm (Chen et al., 2020). The particle-loaded filters used for heterogeneous reactions were prepared according to the procedure used in our previous work (R. Li et al., 2020): (a) approximately 250 mg $CaCO_3$ particles were transferred into 500 mL HPLC-grade ethanol, and the $CaCO_3$/ethanol mixture (0.5 g/L) was stirred using a magnetic stirrer to keep it homogeneous; (b) 10 mL aqueous mixture was transferred onto a PTFE filter (47 mm in diameter, Whatman, USA) to form a particle film on the filter

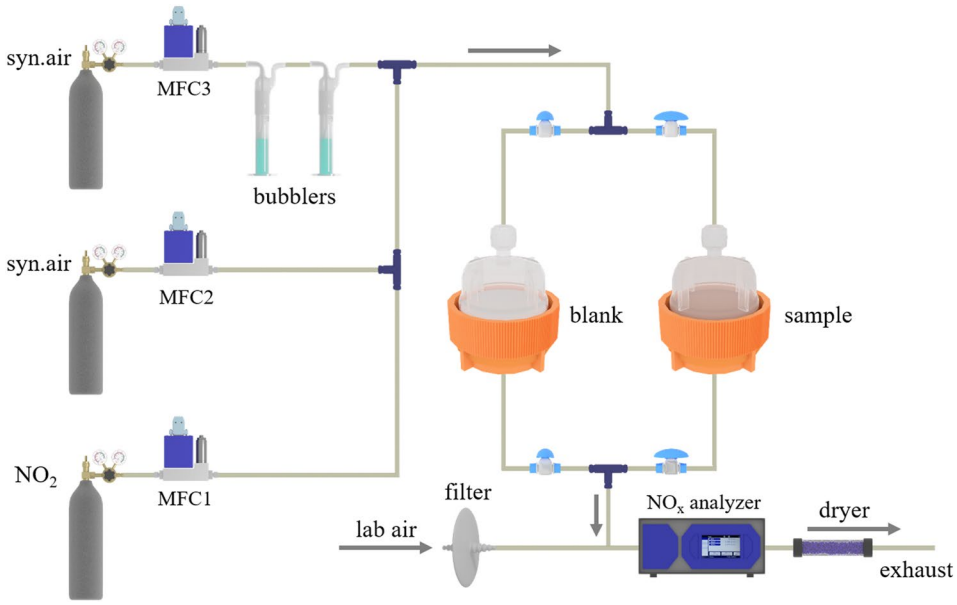

Figure 1. Schematic diagram of the fixed-bed reactor used to study heterogeneous reaction of NO_2 with $CaCO_3$ particles. A blank PTFE filter was housed in the left filter holder, and a particle-loaded filter was housed in the right filter holder.

after ethanol was evaporated; (c) the mass of $CaCO_3$ particles on individual filters prepared was determined to be 5.0 ± 1.0 mg, via measuring the mass of filters before and after $CaCO_3$ particles were loaded. Particles were fairly evenly distributed on the filters, as confirmed by visual inspection.

The density of $CaCO_3$ is 2.93 g/cm^3. If we assume that $CaCO_3$ particles are spherical (with an average diameter of 3.12 μm), it is estimated that <1 layer of particles (around 0.6 layer, to be more precise) was formed on the PTFE filters; nevertheless, some $CaCO_3$ particles deposited on the filter may overlap with each other, thereby potentially shielding some surfaces from NO_2 uptake. In addition, because in our experiments the NO_2 flow was transferred through the particle-loaded filter (see Section 2.1.2), it is justified to assume that all the $CaCO_3$ particles on the filter were exposed to NO_2.

2.1.2. Fixed-Bed Reactor

The fixed-bed reactor used to investigate heterogeneous reaction with NO_2 is similar to that described in our previous work (R. Li et al., 2020), and a brief description is provided here. As shown in Figure 1, three flows, including a dry synthetic air flow (>99.999%, Huate Gas Co., Foshan, China), a humidified synthetic air flow, and a NO_2 flow from a NO_2/air cylinder (1,000 ppmv, National Institute of Metrology, Beijing, China), were mixed in order to obtain desired RH (0%–80%) and NO_2 concentrations (10 ± 0.5 or 2.0 ± 0.1 ppmv, i.e., 2.5×10^{14} or 5.0×10^{13} molecule cm^{-3}). The humidified synthetic airflow was generated by passing a dry synthetic airflow through two water bubblers in series. All the three flows were regulated with mass flow controllers (MFC): the dry and humidified synthetic airflows had a total flow rate of 200 sccm (standard cubic centimeter per minute), and the NO_2 flow was set to 2 or 0.4 sccm.

The following procedure was adopted to investigate heterogeneous reaction of $CaCO_3$ particles with NO_2: (a) the mixed flow was delivered through a blank PTFE filter housed in a fluorinated ethylene propylene (FEP) filter holder (Savillex, Eden Prairie, MN, USA); (b) when the NO_2 concentration was stable, the mixed flow was redirected through a particle-loaded PTFE filter (housed in another FEP filter holder) to initiate the heterogeneous reaction; (c) after a given period (3–24 h, in our work), the mixed flow was delivered through the blank filter again to terminate the reaction, and the particle-loaded filter was taken out from the filter holder and stored in a sealed plastic disk (which was placed in a desiccator) for analysis. The mixed flow exiting the filter holder was diluted by filtered lab air to 500 sccm (cubic centimeter per min) and sampled into a NO/NO_x analyzer (T200, Teledyne Instruments, USA) to monitor NO_2 concentrations with a stated detection limit of 0.4 ppbv, and the measured NO_2 concentrations could be used to calculate

NO_2 concentrations in the filter holder after taking into account the dilution by filtered lab air (diluted by a factor of 2.3). Since NO_2 concentrations were <0.1 ppmv in filtered lab air, the influence of NO_2 contained in filtered lab air on the measured NO_2 concentrations could be neglected. In addition, no difference in measured NO_2 concentrations was observed when the NO_2 flow was passed through the blank filter or through the particle-loaded filter (Figure S1), suggesting that the loss of NO_2 due to its uptake onto $CaCO_3$ was very small in our experiments. All the experiments were conducted at room temperature (24 ± 2°C).

2.2. Measurement of Particle Composition and Hygroscopicity

After heterogeneous reaction with NO_2, the particle-loaded filter was divided into two parts: the first part consisted of 10 filter aliquots (each with a diameter of 4 mm) punched from the original filter, and in this work the remaining part of the original filter was referred to as the second part.

The first part of the filter was first delivered into the sample crucible of a Q5000 vapor sorption analyzer (VSA, TA instruments, Delaware, USA) to examine water uptake as a function of RH. As described in our previous studies (Chen et al., 2020; Gu et al., 2017; M. J. Tang, Zhang, et al., 2019), this instrument measures mass change of samples due to water uptake to determine their hygroscopicity, and the following procedure was employed in this work: (a) the sample was dried at <1% RH; (b) RH was increased to 20%, 40%, 60%, 80%, and 90%; (c) RH was returned to <1% to dry the sample again. When the mass change of the sample was <0.05% in 60 min, we believed that an equilibrium was reached and RH was then changed to the next step. The VSA instrument was routinely calibrated (Chen et al., 2020; Gu et al., 2017), and all the measurements were carried out at 25°C.

The first part (after VSA measurements) and the second part of the filter were separately immersed in 10 mL deionized water, and the mixtures were stirred for 2 h using an oscillating table to extract water soluble inorganic ions (Chen et al., 2020; R. Li et al., 2020). Afterward, 0.22 μm polyethersulfone filters (Anpel, Shanghai, China) were used to filter these extracts, and the resulting solutions were then analyzed using ion chromatography (R. Li et al., 2020) to quantify the amount of nitrate formed. As the VSA instrument is non-destructive, the amount of nitrate formed on a filter is equal to the sum of these formed on the first and second parts of the filter.

To quantify hygroscopicity, one needs to know the mass of dry particles and the mass of water associated with these particles at a given RH. In our work, we could directly measure the amount of particulate water on the first part of a filter and the mass of particles on the entire filter; therefore, we needed to derive the amount of particulate water associated with the entire filter from that associated with the first part of the filter (see Section 3.2 for further details related to the calculation). It would be preferable to directly measure the amount of particulate water on an entire filter; however, this was practically difficult, because sample crucibles used for the VSA instruments were very small. Each crucible was a hemisphere with an inner diameter of ~6 mm; as a result, each time we could only place 10 filter aliquots (each with a diameter of 4 mm), instead of the entire filter, into the crucible.

3. Results and Discussion

3.1. Kinetics of Nitrate Formation and NO_2 Uptake

Figure S1 shows time series of measured NO_2 concentrations (after taking into account the dilution by filtered lab air) in an experiment in which $CaCO_3$ particles were exposed to 10 ppmv NO_2 at 40% RH. As shown in Figure S1, decrease in NO_2 concentrations was very small (even insignificant) when the gas flow was passed through the $CaCO_3$-loaded filter.

After heterogeneous reaction with 10 ppmv NO_2 for 12 h at <1% RH, the mass of nitrate formed relative to the initial mass of $CaCO_3$, noted as $m(NO_3^-)/m_0$, was measured to be (0.11 ± 0.03)%, and increase in reaction time to 24 h did not result in further formation of nitrate. This suggested that at <1% RH, heterogeneous reactivity of $CaCO_3$ toward NO_2 was very low, and $CaCO_3$ surface became completely saturated after exposure to NO_2. If we assume that all the nitrate observed was formed in the first 3 h at <1% RH, $\gamma(NO_2)$ was estimated to be $(2.0 \pm 0.6) \times 10^{-8}$, which was likely to be the upper limit.

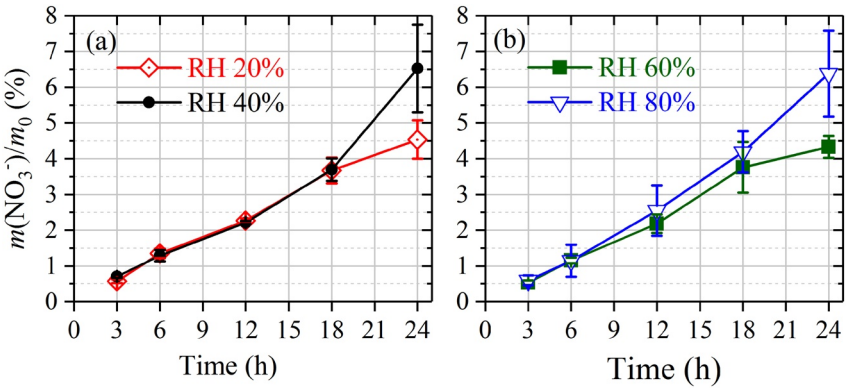

Figure 2. The amounts of nitrate formed, relative to the initial mass of unreacted $CaCO_3$, as a function of time due to heterogeneous reaction with 10 ppmv NO_2 at different relative humidity: (a) 20% and 40%; (b) 60% and 80%.

In contrast, nitrate formation was substantially enhanced at elevated RH (20%–80%). As shown in Figure 2, $m(NO_3^-)/m_0$ increased to >2% after 12 h and to ~5% after 24 h, suggesting that for RH in the range of 20%–80%, reactivity of $CaCO_3$ was not reduced as its reaction with NO_2 proceeded. Similarly, previous studies also found that $CaCO_3$ surface was not saturated after exposure to NO_2 (H. J. Li et al., 2010) at 60%–71% RH and at 40%–85% RH (Tan et al., 2016). As a result, both our current and previous studies (H. J. Li et al., 2010; Tan et al., 2016) suggested that heterogeneous reaction with NO_2 at elevated RH is not limited to $CaCO_3$ surface; to be more specific, uptake of NO_2 at elevated RH led to the formation of an aqueous layer on solid $CaCO_3$, and nitric acid formed in the aqueous layer due to NO_2 uptake would further dissolve $CaCO_3$. Our previous work (R. Li et al., 2020) employed a very similar set-up to examine heterogeneous reactions of NO_2 (15 and 2.5 ppmv) with hematite, goethite and magnetite. It was found that after 24 h or less, these surfaces were significantly or even fully saturated (R. Li et al., 2020), being different from what was observed for $CaCO_3$. In addition to nitrate, nitrite or HONO should also be formed in heterogeneous reaction of NO_2 with $CaCO_3$ (R. Li et al., 2010). In our work, nitrite was not detected in reacted $CaCO_3$ particles, implying that HONO was the other major product.

The change in nitrate with reaction time, as displayed in Figure 2, can be used to calculate the average pseudo-first-order formation rate of nitrate (k_{het}, s^{-1}) in a given period, which is equal to the gas-particle reactive collision frequency:

$$k_{het} = d\left[NO_3^-\right] / dt \tag{1a}$$

The reactive uptake coefficient of NO_2, $\gamma(NO_2)$, defined as ratio of the reactive collision frequency to the total collision frequency (H. J. Li et al., 2010; R. Li et al., 2020; Tan et al., 2016), can thus be determined:

$$\gamma\left(NO_2\right) = k_{het} / Z \tag{1b}$$

The total collision frequency between NO_2 molecules and particles, Z, can be calculated using Equation 1c:

$$Z = 0.25 \cdot A_s \cdot \left[NO_2\right] \cdot c\left(NO_2\right) \tag{1c}$$

where $c(NO_2)$ is the average molecular speed of NO_2 (37,043 cm s^{-1} at 298 K), and $[NO_2]$ is the NO_2 concentration (molecule cm^{-3}). The surface area of $CaCO_3$ particles available for NO_2 uptake, A_s, is equal to the mass (~5 mg) of $CaCO_3$ on the filter multiplied by its BET surface area (2.18 m^2/g), assuming that all the $CaCO_3$ particles on the filter are available for NO_2 uptake. As discussed in Section 2.1.2, even though it is estimated that <1 layer of particles was deposited on the PTFE filter, some particles may still overlap with each other, shielding some surface from NO_2 uptake and causing errors in A_s and thus $\gamma(NO_2)$. It is usually assumed that one nitrate is formed for each two NO_2 molecules removed due to heterogeneous uptake; as a result, $\gamma(NO_2)$ derived from nitrate formation rates, as done in our work, is equal to half of that derived from NO_2 removal rates.

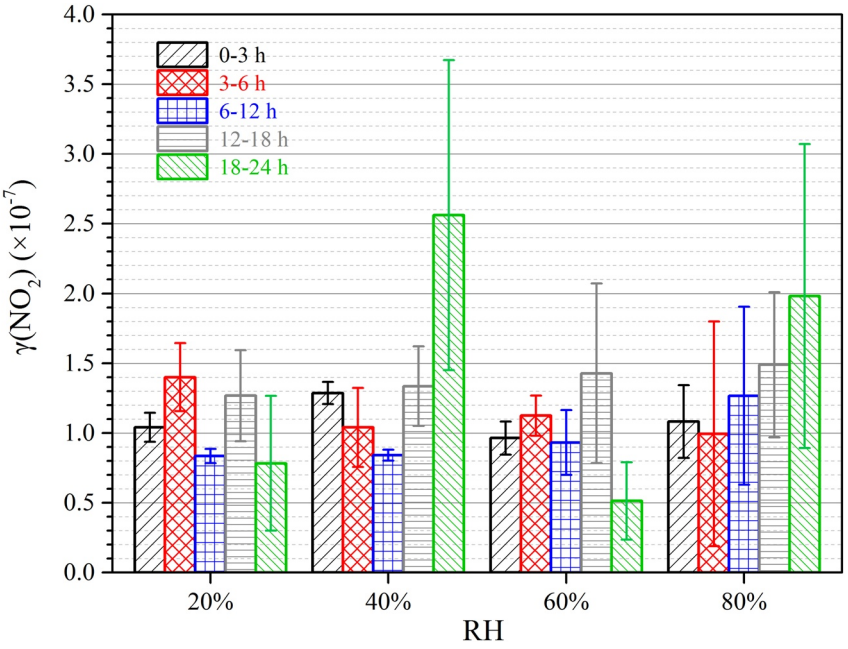

Figure 3. Average uptake coefficients at different periods for heterogeneous reaction of NO_2 (10 ± 0.5 ppmv) with $CaCO_3$ at different relative humidity (20%, 40%, 60%, and 80%).

Figure 3 shows average $\gamma(NO_2)$ at different periods for heterogeneous reaction of 10 ppmv NO_2 with $CaCO_3$ particles as a function of RH (20%–80%). Taking into account the experimental uncertainties, two features can be observed from the results displayed in Figure 3. First, at each individual RH, there was no systematical variation of $\gamma(NO_2)$ with reaction time, because the amount of nitrate formed increased almost linearly with reaction time (see Figure 2). Second, no change in $\gamma(NO_2)$ was observed when RH was increased from 20% to 80%. Taking all the data together, the average $\gamma(NO_2)$ was determined to be $(1.21 \pm 0.45) \times 10^{-7}$ for $CaCO_3$ when the NO_2 concentration was 10 ppmv, independent of RH (20%–80%) and reaction time (3–24 h), and it was at least a factor of six larger than that at <1% RH ($\sim 2 \times 10^{-8}$).

3.1.1. Effects of NO_2 Concentrations

In order to explore the effects of NO_2 concentrations, we also investigated heterogeneous reaction of $CaCO_3$ with NO_2 at a lower NO_2 concentration (2 ± 0.1 ppmv). Figure S2 shows the amounts of nitrate formed at 40% and 80% RH as a function of reaction time, suggesting that the amount of nitrate formed also increased linearly with time at both RH. The average $\gamma(NO_2)$, independent of RH (40% and 80%) and reaction time (3–24 h), was determined to be $(1.38 \pm 0.41) \times 10^{-7}$ when NO_2 concentration was 2 ppmv; for comparison, the average $\gamma(NO_2)$ was measured to be $(1.21 \pm 0.45) \times 10^{-7}$ when NO_2 concentration was 10 ppmv. Therefore, one may conclude that essentially no change (or slight increase) in $\gamma(NO_2)$ was observed when NO_2 concentrations were decreased from ~10 to ~2 ppmv (by a factor of five).

Our previous work (R. Li et al., 2020) studied heterogeneous reactions of three iron (hydro)oxides with NO_2 at a similar concentration (2.5 ppmv, i.e., $\sim 6.2 \times 10^{13}$ molecule cm^{-3}), and the initial $\gamma(NO_2)$ at 30%–90% RH was determined to be $(1.2–1.4) \times 10^{-8}$ for hematite, $(2.7–2.9) \times 10^{-8}$ for magnetite and $(4.0–4.8) \times 10^{-8}$ for goethite, all significantly smaller than that for $CaCO_3$. This suggests that when compared to hematite, magnetite and goethite, $CaCO_3$ exhibits higher heterogeneous reactivity toward NO_2.

3.1.2. Comparison With Previous Studies

Initial $\gamma(NO_2)$ values, reported by previous studies (H. J. Li et al., 2010; Tan et al., 2016), are also listed in Table 1, in order to be compared with these determined in our work. The most striking feature revealed by such comparison is that at elevated RH (20% or higher), $\gamma(NO_2)$ reported by our work is ~50 times larger than those reported by other studies. NO_2 concentrations used in our work was 1–2 orders of magnitude lower

Table 1
Initial $\gamma(NO_2)$ Onto $CaCO_3$ Particles: Comparison of Our Work With Previous Studies (H. J. Li et al., 2010; Tan et al., 2016)

$[NO_2]$	RH	$\gamma(NO_2)$	References
$(6.9–16.8) \times 10^{15}$	<10%	$(4.25 \pm 1.18) \times 10^{-9}$	H. J. Li et al. (2010)
$(4.6–11.4) \times 10^{15}$	60%–71%	$(2.54 \pm 0.13) \times 10^{-9}$	
2.6×10^{15}	<1%	$(3.34 \pm 0.14) \times 10^{-9}$	Tan et al. (2016)
	40%	$(2.04 \pm 0.07) \times 10^{-9}$	
	60%	$(2.23 \pm 0.22) \times 10^{-9}$	
	85%	$(2.28 \pm 0.17) \times 10^{-9}$	
2.5×10^{14}	<1%	$<2 \times 10^{-8}$	This work
	20%	$(1.04 \pm 0.10) \times 10^{-7}$	
	40%	$(1.29 \pm 0.08) \times 10^{-7}$	
	60%	$(0.96 \pm 0.12) \times 10^{-7}$	
	80%	$(1.08 \pm 0.26) \times 10^{-7}$	
5.0×10^{13}	40%	$(1.55 \pm 0.19) \times 10^{-7}$	
	80%	$(1.38 \pm 0.28) \times 10^{-7}$	

Note. $[NO_2]$: NO_2 Concentrations in Molecule cm^{-3}

than those used in other studies (H. J. Li et al., 2010; Tan et al., 2016); however, the difference in NO_2 concentrations used is unlikely to fully explain the large discrepancy in reported $\gamma(NO_2)$.

All the three studies assumed that all the surfaces of $CaCO_3$ particles were available for NO_2 uptake. However, the two previous studies (H. J. Li et al., 2010; Tan et al., 2016) placed multiple layers of $CaCO_3$ particles into samples holders, and $CaCO_3$ particles in the underlying layers might not be accessible by NO_2 molecules. As a result, the two previous studies could significantly overestimate surface areas actually available for heterogeneous reaction and consequently underestimate uptake coefficients. As pointed out by Tan et al. (2016), if the surface area available for NO_2 uptake was assumed to be the geometric surface area of their sample holder, the calculated $\gamma(NO_2)$ would be approximately three orders of magnitude larger.

Instead of using multiple layers of particles, in our work we deposited $CaCO_3$ particles onto PTFE filters in such a way that less than one layer of particles were deposited on each filter, through which the NO_2 flow was delivered. Hence it is reasonable to expect that most of the particles, if not all, would be truly exposed to NO_2. This explains why $\gamma(NO_2)$ reported in our work are ~50 times larger than those reported in previous studies (H. J. Li et al., 2010; Tan et al., 2016), and assures that $\gamma(NO_2)$ reported in our work are more reliable. Because there is still the possibility that some of particles used in our work, as being deposited on filters, may not be available for heterogeneous uptake, true $\gamma(NO_2)$ would be larger than those reported in our work. In other words, $\gamma(NO_2)$ determined in our work should still be considered as the lower limit. However, compared to previous studies (H. J. Li et al., 2010; Tan et al., 2016), our work has raised the lower limit by a factor of ~50 and thus would significantly reduce the uncertainty of $\gamma(NO_2)$ for $CaCO_3$.

3.2. Change in Hygroscopicity of $CaCO_3$ Particles

Because sample crucibles of the VSA instrument were very small (see Section 2.2), we could only directly measure water uptake by the first part of a particle-loaded filter (i.e., 10 pieces of 4 mm filter aliquots). Here we use a $CaCO_3$-loaded filter after heterogeneous reaction with 10 ppmv NO_2 at 40% RH for 24 h as an example, to illustrate how we can derive the amount of water on the entire $CaCO_3$-loaded filter. As shown in Figure 4a, the mass of particulate water on the first part of the filter was measured to be 0.0222, 0.0420, 0.0683, 0.1307, and 0.2403 mg at 20%, 40%, 60%, 80%, and 90% RH.

The ratio of nitrate formed on the entire filter to that formed on the first part of the filter, as measured using ion chromatography, was determined to be 11.64. Since the amount of water on the unreacted $CaCO_3$-loaded filter was negligible (see Figure 5a), one could conclude that water uptake by reacted $CaCO_3$-loaded filter was solely determined by nitrate formed in heterogeneous reaction with NO_2. Therefore, the ratio of particulate water on the entire filter to that on the first part of the filter was also equal to 11.64. Consequently, we could derive the mass of particulate water on the entire filter from the data displayed in Figure 4a. Furthermore, as we know the initial mass of unreacted $CaCO_3$ particles on the filter (5.0 mg), the relative mass of particulate water, normalized to the initial mass of unreacted $CaCO_3$, could also be derived, and the result is displayed in Figure 4b.

Figure 5b shows water uptake by the first part of a $CaCO_3$-loaded filter after heterogeneous reaction with 10 ppmv NO_2 for 24 h at <1% RH. It is evident from Figure 5b that heterogeneous reaction with NO_2 at <1% RH did not lead to observable increase in hygroscopicity of $CaCO_3$. This is expectable because the amount of nitrate formed on $CaCO_3$ was insignificant after heterogeneous reaction with 10 ppmv NO_2 for 24 h at <1% RH (see Section 3.1).

Hygroscopic growth of reacted $CaCO_3$, exposed to 10 ppmv NO_2 for 24 h at 40% RH, is displayed as an example in Figure 4b, in which ratios of the mass of particulate water to the initial mass of unreacted $CaCO_3$,

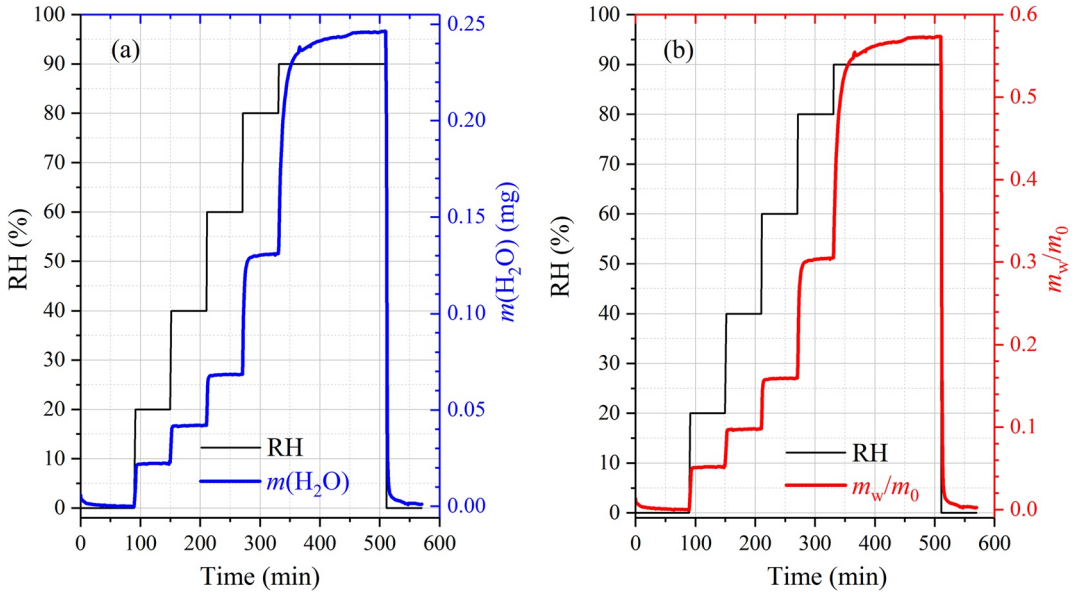

Figure 4. (a) Change in mass of particulate water on the first part of a $CaCO_3$-loaded filter as a function of relative humidity (RH), after heterogeneous reaction with 10 ppmv NO_2 for 24 h at 40% RH. (b) Change in relative mass of particulate water (relative to the initial mass of unreacted $CaCO_3$ particles) as a function of RH on the same filter.

m_w/m_0, are plotted as a function of RH. For reacted $CaCO_3$ shown in Figure 4b, m_w/m_0 was measured to be ~0.052 at 20% RH, ~0.159 at 60% RH and 0.573 at 90% RH. In comparison, m_w/m_0 was determined to be <0.002 at 90% RH for unreacted $CaCO_3$ in our previous work (Chen et al., 2020), suggesting heterogeneous reaction of $CaCO_3$ with NO_2 at 40% RH led to significant increase in its hygroscopicity. As also revealed by Figure 4, reacted $CaCO_3$ particles started to take up substantial amount of water even at 20% RH, while the deliquescence RH of $Ca(NO_3)_2{\cdot}4H_2O$ is ~50% (Guo et al., 2019; Kelly & Wexler, 2005). This observation indicates that $Ca(NO_3)_2$ formed due to heterogeneous uptake of NO_2 onto $CaCO_3$ was amorphous and thus could take up significant amounts of water at very low RH, in consistent with previous work (Al-Abadleh et al., 2003; Y. J. Liu et al., 2008; I. N. Tang & Fung, 1997).

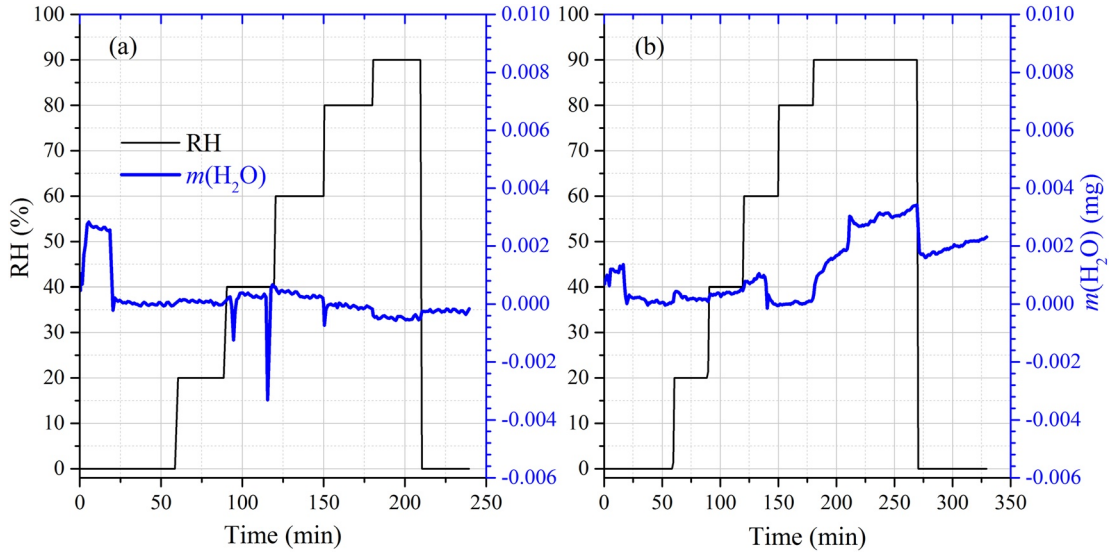

Figure 5. Change in mass of particulate water as a function of relative humidity (RH) for the first part of (a) an unreacted $CaCO_3$-loaded filter and (b) a $CaCO_3$-loaded filter after heterogeneous reaction with 10 ppmv NO_2 for 24 h at <1% RH.

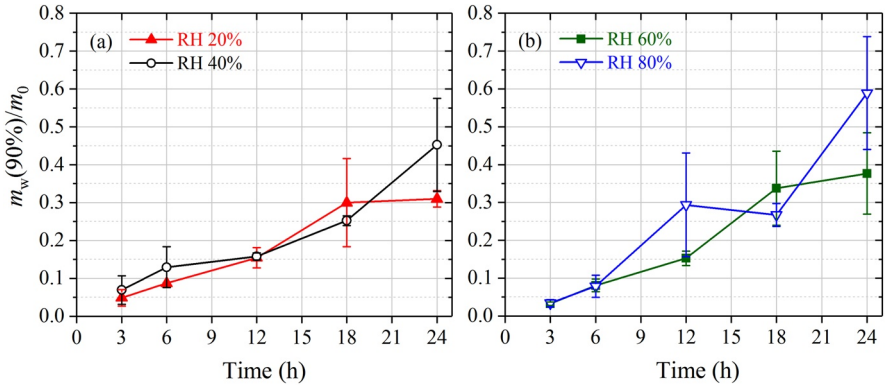

Figure 6. Changes in hygroscopicity of $CaCO_3$ with reaction time after heterogeneous reaction with 10 ppmv NO_2 at different relative humidity (RH, 20%, 40%, 60%, and 80%). Here hygroscopicity is represented by $m_w(90\%)/m_0$, that is, the relative mass of particulate water at 90% RH (normalized to the mass of unreacted $CaCO_3$).

Significant increase in hygroscopicity was also observed for reacted $CaCO_3$ after heterogeneous reaction with 10 ppmv NO_2 for shorter periods (3–24 h) and at other RH (20%, 60%, and 80%). Below we focus our discussion on hygroscopic properties of reacted $CaCO_3$ (after reaction with NO_2 at different RH for different periods) at 90% RH, that is, $m_w(90\%)/m_0$, which is defined as the ratio of the mass of particulate water of reacted $CaCO_3$ at 90% RH to the initial mass of unreacted $CaCO_3$.

As shown in Figure 6, heterogeneous reaction with NO_2 at 20%–80% RH caused significant increase in hygroscopic properties of $CaCO_3$ particles. Take the reaction at 40% RH as an example: prior to NO_2 uptake, $m_w(90\%)/m_0$ was only 0.002 for $CaCO_3$; however, as shown in Figure 6a, it increased to 0.040 ± 0.012, 0.125 ± 0.035, and 0.452 ± 0.123 after reaction with NO_2 for 3, 12, and 24 h. In other word, after reaction with 10 ppmv NO_2 for 24 h at 40% RH, the mass of particulate water associated with reacted $CaCO_3$ was equal to ~45% of the initial mass of unreacted $CaCO_3$. Figure 6 further suggests that when the relatively large experimental uncertainties are considered, $m_w(90\%)/m_0$ was similar for reacted $CaCO_3$ after reaction with NO_2 for a given time at different RH (20%–80%). This is because the formation rates of nitrate did not vary significantly for RH in the range of 20%–80%, as discussed in Section 3.1.

The single hygroscopicity parameter, κ, is widely used to represent aerosol hygroscopicity (Peng et al., 2020; Petters & Kreidenweis, 2007; M. J. Tang et al., 2016), and the κ value was determined to be <0.01 for unreacted $CaCO_3$ (Sullivan et al., 2009a; M. J. Tang et al., 2015; Zhao et al., 2010). If we assume that the particle volume at 90% RH is equal to the sum of dry particle volume and the volume of water and that the Kelvin effect is negligible, Equation 2 can be used to calculate κ (Guo et al., 2020; M. J. Tang, Gu, et al., 2019):

$$\kappa = \frac{m_w}{m_0} \cdot \frac{\rho_0}{\rho_w} \cdot \frac{1 - 0.9}{0.9} \tag{2}$$

where m_w is the mass of water at 90% RH, m_0 is the dry particle mass, ρ_w is the density of water, and ρ_0 is the dry particle density. Here m_0 is assumed to be the mass of unreacted $CaCO_3$ and ρ_0 is assumed to be the density of $CaCO_3$ (2.93 g/cm^3). As displayed in Figure 6, after heterogeneous reaction with 10 ppmv NO_2 at 20%–80% RH for 24 h, m_w/m_0 at 90% RH increased to ~0.4 for reacted $CaCO_3$, and the corresponding κ value was estimated to be ~0.13.

3.3. Discussion

For unreacted and reacted $CaCO_3$ particles, we also measured their hygroscopic properties at 20%, 40%, 60%, and 80% RH, in addition to 90% RH. As heterogeneous reaction with NO_2 was also examined at 20%, 40%, 60%, and 80% RH, we could thus monitor changes in nitrate and particulate water as a function of time during NO_2 uptake at each RH.

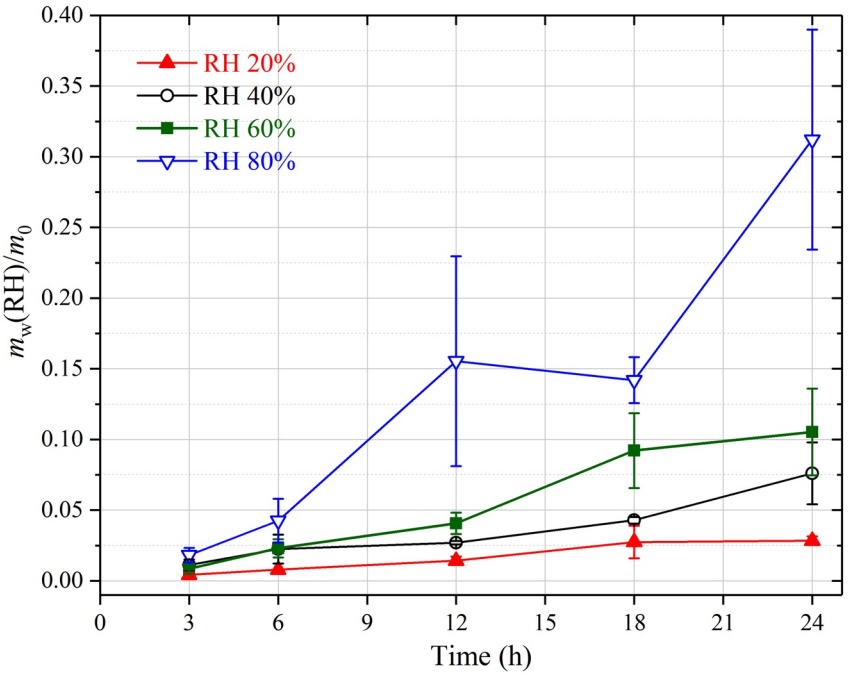

Figure 7. Changes in relative mass of particulate water (normalized to the initial mass of unreacted $CaCO_3$) of reacted $CaCO_3$ as a function of time during heterogeneous reaction with 10 ppmv NO_2 at different relative humidity (20%, 40%, 60%, and 80%).

Figure 7 displays changes in particulate water with time for heterogeneous reaction with 10 ppmv NO_2 at 20%, 40%, 60%, and 80% RH, and two interesting features can be identified. First, for heterogeneous reaction with NO_2 at a given RH, the amount of particulate water would increase with reaction time. For example, during heterogeneous reaction with NO_2 at 40% RH, the relative mass of particulate water (m_w/m_0, relative to the initial mass of unreacted $CaCO_3$), increased to 0.011 ± 0.004, 0.027 ± 0.001, and 0.076 ± 0.022 after reaction for 3, 12, and 24 h. This is simply because the amount of nitrate formed increased with reaction time. Second, while the amount of nitrate formed was very similar at different RH (20%–80%) for a given reaction time (shown in Figure 2), the amount of particulate water would increase substantially with RH. For example, after reaction with 10 ppmv NO_2 for 24 h, m_w/m_0 was determined to be 0.028 ± 0.003 at 20% RH, 0.076 ± 0.022 at 40% RH, 0.105 ± 0.031 at 60% RH, and 0.312 ± 0.078 at 80%, respectively. This can be expected because for the same amount of nitrate, the amount of particulate water would increase with RH.

Even under dry conditions, some adsorbed water can still remain on the surface of $CaCO_3$ and dissociate to form $Ca(OH)(HCO_3)$ (Al-Hosney & Grassian, 2004, 2005). Therefore, $CaCO_3$ particles would be covered with surface OH groups, which provide reactive surface sites of NO_2 uptake (H. J. Li et al., 2010). After these reactive sites are consumed due to NO_2 uptake under dry conditions, $CaCO_3$ surface would be saturated and hence the formation of nitrate is very limited at <1% RH, as observed in our work (see Section 3.1). Nevertheless, if heterogeneous reaction with NO_2 takes place at elevated RH (20%–80% in our work), nitrate formed on $CaCO_3$ particles would take up water and become deliquesced, and thus reacted $CaCO_3$ would be covered with an aqueous layer which would sustain NO_2 uptake. Uptake of NO_2 by this aqueous layer would lead to the formation of HNO_3, which would further dissolve $CaCO_3$; as a result, as the reaction proceeds at elevated RH, the amounts of nitrate and particulate water would increase, as observed in our work.

It is suggested that NO_2 uptake onto water surfaces is driven by heterogeneous hydrolysis of NO_2, and the corresponding $\gamma(NO_2)$ can be calculated using Equation 3 (Ammann et al., 2013):

$$\gamma\left(NO_2\right) = \frac{4HRT}{c\left(NO_2\right)}\sqrt{D_l \cdot H \cdot \left[NO_2\right] \cdot k_l} \quad (3)$$

where H is the Henry's law constant of NO_2, R is the gas constant, T is temperature, $c(NO_2)$ is the average molecular speed of NO_2, D_l is the diffusion coefficient of NO_2 molecules in liquid water, $[NO_2]$ is the NO_2 concentration in the gas phase, and k_l is the aqueous phase rate constant. Using Equation 3, $\gamma(NO_2)$ is calculated to be $\sim 6 \times 10^{-9}$ at 10 ppbv NO_2 (Ammann et al., 2013). Therefore, when NO_2 concentration is 10 ppmv, $\gamma(NO_2)$ is estimated to be $\sim 1.9 \times 10^{-7}$ for water surfaces, in fairly good agreement with that determined in our work ($\sim 1.2 \times 10^{-7}$) for heterogeneous uptake of NO_2 onto $CaCO_3$ at 20%–80% RH. This provides further support to our proposed mechanism that heterogeneous reaction of NO_2 with $CaCO_3$ at elevated RH is driven by heterogeneous hydrolysis of NO_2 in the deliquesced layer formed on $CaCO_3$ particles.

4. Conclusions

Heterogeneous reaction of NO_2 with $CaCO_3$, an important component in mineral dust aerosol, may be a non-negligible source for HONO, and also leads to the formation of nitrate and thus increase in aerosol hygroscopicity. However, uptake coefficients of this reaction, reported in previous studies, may have large uncertainties, and the interactions between heterogeneous reactivity and hygroscopicity, have not been elucidated. In our work, a fixed-bed reactor was employed to investigate heterogeneous reaction of NO_2 with $CaCO_3$ at different RH (0%–80%), and changes in particulate nitrate and water were determined as a function of reaction time (3–24 h).

When NO_2 concentration was 10 ppmv ($\sim 2.5 \times 10^{14}$ molecule cm^{-3}), heterogeneous reactivity of $CaCO_3$ toward NO_2 was found to be very low at <1% RH, and $\gamma(NO_2)$ was estimated to $< 2 \times 10^{-8}$. Increase in RH to 20% or higher would substantially promote heterogeneous uptake of NO_2 onto $CaCO_3$, and no surface saturation was observed after reaction for 24 h; the average $\gamma(NO_2)$ was determined to be $(1.21 \pm 0.45) \times 10^{-7}$, independent of RH (20%–80%) and reaction time (3–24 h). We found that during heterogeneous reaction with NO_2 at 20%–80% RH, reacted $CaCO_3$ took up considerable amounts of water due to the formation of nitrate, and therefore would be covered by a deliquesced $Ca(NO_3)_2/H_2O$ layer, which further drove NO_2 uptake via heterogeneous hydrolysis. This can explain why no dependence of $\gamma(NO_2)$ on RH (20%–80%) or reaction time (3–24 h) was observed. In addition, no significant change (or a slight increase) in $\gamma(NO_2)$ at 40% and 80% RH was observed when NO_2 concentration was reduced by a factor or five, from 2.5×10^{14} to 5.0×10^{13} molecule cm^{-3} (i.e., from 10 to 2 ppmv).

No significant change in hygroscopicity of $CaCO_3$ particles was observed after exposure to 10 ppmv NO_2 at <1% RH, because the amount of nitrate formed was very small. Heterogeneous reaction of $CaCO_3$ with 10 ppmv NO_2 at 20%–80% RH could significantly increase its hygroscopicity. For example, after reaction with 10 ppmv NO_2 for 24 h at 20%–80% RH, the mass of particulate water associated with reacted $CaCO_3$ at 90% RH was equal to ~45% of the initial mass of unreacted $CaCO_3$. As we determined changes in composition and hygroscopicity of $CaCO_3$ due to heterogeneous reaction with NO_2 as a function of reaction time at different RH, the quantitative and systematic data set obtained in our work can help us better understand the hygroscopicity of $CaCO_3$ particles during transport in the troposphere. It should be pointed out that NO_2 concentrations (2.5–10 ppmv) used in our study were significantly higher than those in the troposphere. In addition, although concentrations of HNO_3 and N_2O_5 in the troposphere are lower than NO_2, their heterogeneous reactivity toward mineral dust is much higher (Crowley et al., 2010); as a result, heterogeneous reactions of HNO_3 and N_2O_5 may substantially increase hygroscopicity of $CaCO_3$ particles and should be investigated in future.

Conflict of Interest

The authors declare no conflicts of interest relevant to this study.

Data Availability Statement

Data supporting this paper can be found at http://doi.org/10.5281/zenodo.4733826.

Acknowledgments
This work was funded by National Natural Science Foundation of China (42022050 and 91744204), State Environmental Protection Key Laboratory of Formation and Prevention of Urban Air Pollution Complex (CX2020080094), Guangdong Basic and Applied Basic Research Fund Committee (2020B1515130003), Guangdong Foundation for Program of Science and Technology Research (2019B121205006 and 2020B1212060053), Guangdong Science and Technology Department (2017GC010501) and CAS Pioneer Hundred Talents program.

References

Al-Abadleh, H. A., Krueger, B. J., Ross, J. L., & Grassian, V. H. (2003). Phase transitions in calcium nitrate thin films. *Chemical Communications*, 2796–2797. https://doi.org/10.1039/b308632a

Al-Hosney, H. A., & Grassian, V. H. (2004). Carbonic acid: An important intermediate in the surface chemistry of calcium carbonate. *Journal of the American Chemical Society*, *126*, 8068–8069. https://doi.org/10.1021/ja0490774

Al-Hosney, H. A., & Grassian, V. H. (2005). Water, sulfur dioxide and nitric acid adsorption on calcium carbonate: A transmission and ATR-FTIR study. *Physical Chemistry Chemical Physics*, *7*, 1266–1276. https://doi.org/10.1039/b417872f

Ammann, M., Cox, R. A., Crowley, J. N., Jenkin, M. E., Mellouki, A., Rossi, M. J., et al. (2013). Evaluated kinetic and photochemical data for atmospheric chemistry: Volume VI—Heterogeneous reactions with liquid substrates. *Atmospheric Chemistry and Physics*, *12*, 8045–8228. https://doi.org/10.5194/acp-13-8045-2013

Angelini, M. M., Garrard, R. J., Rosen, S. J., & Hinrichs, R. Z. (2007). Heterogeneous reactions of gaseous HNO_3 and NO_2 on the clay minerals kaolinite and pyrophyllite. *The Journal of Physical Chemistry A*, *111*, 3326–3335. https://doi.org/10.1021/jp0672656

Borensen, C., Kirchner, U., Scheer, V., Vogt, R., & Zellner, R. (2000). Mechanism and kinetics of the reactions of NO_2 or HNO_3 with alumina as a mineral dust model compound. *The Journal of Physical Chemistry A*, *104*, 5036–5045. https://doi.org/10.1021/jp994170d

Chen, L. X. D., Peng, C., Gu, W. J., Fu, H. J., Jian, X., Zhang, H. H., et al. (2020). On mineral dust aerosol hygroscopicity. *Atmospheric Chemistry and Physics*, *20*, 13611–13626. https://doi.org/10.5194/acp-20-13611-2020

Crowley, J. N., Ammann, M., Cox, R. A., Hynes, R. G., Jenkin, M. E., Mellouki, A., et al. (2010). Evaluated kinetic and photochemical data for atmospheric chemistry: Volume V—Heterogeneous reactions on solid substrates. *Atmospheric Chemistry and Physics*, *10*, 9059–9223. https://doi.org/10.5194/acp-10-9059-2010

Dentener, F. J., Carmichael, G. R., Zhang, Y., Lelieveld, J., & Crutzen, P. J. (1996). Role of mineral aerosol as a reactive surface in the global troposphere. *Journal of Geophysical Research: Atmospheres*, *101*, 22869–22889. https://doi.org/10.1029/96jd01818

El Zein, A., & Bedjanian, Y. (2012). Interaction of NO_2 with TiO_2 surface under UV irradiation: Measurements of the uptake coefficient. *Atmospheric Chemistry and Physics*, *12*, 1013–1020. https://doi.org/10.5194/acp-12-1013-2012

Gibson, E. R., Hudson, P. K., & Grassian, V. H. (2006). Physicochemical properties of nitrate aerosols: Implications for the atmosphere. *The Journal of Physical Chemistry A*, *110*, 11785–11799. https://doi.org/10.1021/jp063821k

Ginoux, P., Prospero, J. M., Gill, T. E., Hsu, N. C., & Zhao, M. (2012). Global-scale attribution of anthropogenic and natural dust sources and their emission rates based on MODIS deep blue aerosol products. *Reviews of Geophysics*, *50*, RG3005. https://doi.org/10.1029/2012rg000388

Guo, L. Y., Gu, W. J., Peng, C., Wang, W. G., Li, Y. J., Zong, T. M., et al. (2019). A comprehensive study of hygroscopic properties of calcium- and magnesium-containing salts: Implication for hygroscopicity of mineral dust and sea salt aerosols. *Atmospheric Chemistry and Physics*, *19*, 2115–2133. https://doi.org/10.5194/acp-19-2115-2019

Guo, L. Y., Peng, C., Zong, T. M., Gu, W. J., Ma, Q. X., Wu, Z. J., et al. (2020). Comprehensive characterization of hygroscopic properties of methanesulfonates. *Atmospheric Environment*, *224*, 117349. https://doi.org/10.1016/j.atmosenv.2020.117349

Gustafsson, R. J., Orlov, A., Badger, C. L., Griffiths, P. T., Cox, R. A., & Lambert, R. M. (2005). A comprehensive evaluation of water uptake on atmospherically relevant mineral surfaces: DRIFT spectroscopy, thermogravimetric analysis and aerosol growth measurements. *Atmospheric Chemistry and Physics*, *5*, 3415–3421. https://doi.org/10.5194/acp-5-3415-2005

Gu, W. J., Li, Y. J., Zhu, J. X., Jia, X. H., Lin, Q. H., Zhang, G. H., et al. (2017). Investigation of water adsorption and hygroscopicity of atmospherically relevant particles using a commercial vapor sorption analyzer. *Atmospheric Measurement Techniques*, *10*, 3821–3832. https://doi.org/10.5194/amt-10-3821-2017

Hatch, C. D., Gierlus, K. M., Schuttlefield, J. D., & Grassian, V. H. (2008). Water adsorption and cloud condensation nuclei activity of calcite and calcite coated with model humic and fulvic acids. *Atmospheric Environment*, *42*(22), 5672–5684. https://doi.org/10.1016/j.atmosenv.2008.03.005

Journet, E., Balkanski, Y., & Harrison, S. P. (2014). A new data set of soil mineralogy for dust-cycle modeling. *Atmospheric Chemistry and Physics*, *14*, 3801–3816. https://doi.org/10.5194/acp-14-3801-2014

Kelly, J. T., & Wexler, A. S. (2005). Thermodynamics of carbonates and hydrates related to heterogeneous reactions involving mineral aerosol. *Journal of Geophysical Research: Atmospheres*, *110*, D11201. https://doi.org/10.1029/2004jd005583

Krueger, B. J., Grassian, V. H., Laskin, A., & Cowin, J. P. (2003). The transformation of solid atmospheric particles into liquid droplets through heterogeneous chemistry: laboratory insights into the processing of calcium containing mineral dust aerosol in the troposphere. *Geophysical Research Letters*, *30*, 1148. https://doi.org/10.1029/2002gl016563

Kumar, R., Barth, M. C., Madronich, S., Naja, M., Carmichael, G. R., Pfister, G. G., et al. (2014). Effects of dust aerosols on tropospheric chemistry during a typical pre-monsoon season dust storm in northern India. *Atmospheric Chemistry and Physics*, *14*(13), 6813–6834. https://doi.org/10.5194/acp-14-6813-2014

Laskin, A., Iedema, M. J., Ichkovich, A., Graber, E. R., Taraniuk, I., & Rudich, Y. (2005). Direct observation of completely processed calcium carbonate dust particles. *Faraday Discussions*, *130*, 453–468. https://doi.org/10.1039/b417366j

Li, H. J., Zhu, T., Zhao, D. F., Zhang, Z. F., & Chen, Z. M. (2010). Kinetics and mechanisms of heterogeneous reaction of NO_2 on $CaCO_3$ surfaces under dry and wet conditions. *Atmospheric Chemistry and Physics*, *10*, 463–474. https://doi.org/10.5194/acp-10-463-2010

Li, J., Wang, Z. F., Zhuang, G., Luo, G., Sun, Y., & Wang, Q. (2012). Mixing of Asian mineral dust with anthropogenic pollutants over East Asia: A model case study of a super-duststorm in March 2010. *Atmospheric Chemistry and Physics*, *12*, 7591–7607. https://doi.org/10.5194/acp-12-7591-2012

Li, R., Jia, X. H., Wang, F., Ren, Y., Wang, X., Zhang, H. H., et al. (2020). Heterogeneous reaction of NO_2 with hematite, goethite and magnetite: Implications for nitrate formation and iron solubility enhancement. *Chemosphere*, *242*, 125273. https://doi.org/10.1016/j.chemosphere.2019.125273

Li, W. J., & Shao, L. Y. (2009). Observation of nitrate coatings on atmospheric mineral dust particles. *Atmospheric Chemistry and Physics*, *9*, 1863–1871. https://doi.org/10.5194/acp-9-1863-2009

Liu, C., Ma, Q. X., He, H., He, G. Z., Ma, J. Z., Liu, Y. C., & Wu, Y. (2017). Structure-activity relationship of surface hydroxyl groups during NO_2 adsorption and transformation on TiO_2 nanoparticles. *Environmental Sciences: Nano*, *4*, 2388–2394. https://doi.org/10.1039/c7en00920h

Liu, Y., Han, C., Ma, J., Bao, X., & He, H. (2015). Influence of relative humidity on heterogeneous kinetics of NO_2 on kaolin and hematite. *Physical Chemistry Chemical Physics*, *17*, 19424–19431. https://doi.org/10.1039/c5cp02223a

Liu, Y. J., Zhu, T., Zhao, D. F., & Zhang, Z. F. (2008). Investigation of the hygroscopic properties of $Ca(NO_3)_2$ and internally mixed $Ca(NO_3)_2/CaCO_3$ particles by micro-Raman spectrometry. *Atmospheric Chemistry and Physics*, *8*, 7205–7215. https://doi.org/10.5194/acp-8-7205-2008

Ma, Q. X., Liu, Y. C., Liu, C., & He, H. (2012). Heterogeneous reaction of acetic acid on MgO, α-Al_2O_3, and $CaCO_3$ and the effect on the hygroscopic behavior of these particles. *Physical Chemistry Chemical Physics*, *14*, 8403–8409. https://doi.org/10.1039/c2cp40510e

Matsuki, A., Iwasaka, Y., Shi, G. Y., Zhang, D. Z., Trochkine, D., Yamada, M., et al. (2005). Morphological and chemical modification of mineral dust: Observational insight into the heterogeneous uptake of acidic gases. *Geophysical Research Letters*, *32*, L22806. https://doi.org/10.1029/2005gl024176

Ndour, M., D'Anna, B., George, C., Ka, O., Balkanski, Y., Kleffmann, J., et al. (2008). Photoenhanced uptake of NO_2 on mineral dust: Laboratory experiments and model simulations. *Geophysical Research Letters*, *35*, L05812. https://doi.org/10.1029/2007gl032006

Nickovic, S., Vukovic, A., Vujadinovic, M., Djurdjevic, V., & Pejanovic, G. (2012). Technical note: High-resolution mineralogical database of dust-productive soils for atmospheric dust modeling. *Atmospheric Chemistry and Physics*, *12*, 845–855. https://doi.org/10.5194/acp-12-845-2012

Pan, X., Ge, B., Wang, Z., Tian, Y., Liu, H., Wei, L., et al. (2019). Synergistic effect of water-soluble species and relative humidity on morphological changes in aerosol particles in the Beijing megacity during severe pollution episodes. *Atmospheric Chemistry and Physics*, *19*, 219–232. https://doi.org/10.5194/acp-19-219-2019

Peng, C., Wang, Y., Wu, Z. J., Chen, L. X. D., Huang, R. J., Wang, W. G., et al. (2020). Tropospheric aerosol hygroscopicity in China. *Atmospheric Chemistry and Physics*, *20*, 13877–13903. https://doi.org/10.5194/acp-20-13877-2020

Petters, M. D., & Kreidenweis, S. M. (2007). A single parameter representation of hygroscopic growth and cloud condensation nucleus activity. *Atmospheric Chemistry and Physics*, *7*, 1961–1971. https://doi.org/10.5194/acp-7-1961-2007

Prospero, J. M., & Mayol-Bracero, O. L. (2013). Understanding the transport and impact of African dust on the Caribbean Basin. *Bulletin of the American Meteorological Society*, *94*(9), 1329–1337. https://doi.org/10.1175/bams-d-12-00142.1

Scanza, R. A., Mahowald, N., Ghan, S., Zender, C. S., Kok, J. F., Liu, X., et al. (2015). Modeling dust as component minerals in the community atmosphere model: Development of framework and impact on radiative forcing. *Atmospheric Chemistry and Physics*, *15*(1), 537–561. https://doi.org/10.5194/acp-15-537-2015

Shi, Z., Zhang, D., Hayashi, M., Ogata, H., Ji, H., & Fujiie, W. (2008). Influences of sulfate and nitrate on the hygroscopic behavior of coarse dust particles. *Atmospheric Environment*, *42*(4), 822–827. https://doi.org/10.1016/j.atmosenv.2007.10.037

Sullivan, R. C., Minambres, L., DeMott, P. J., Prenni, A. J., Carrico, C. M., Levin, E. J. T., & Kreidenweis, S. M. (2010). Chemical processing does not always impair heterogeneous ice nucleation of mineral dust particles. *Geophysical Research Letters*, *37*, L24805. https://doi.org/10.1029/2010gl045540

Sullivan, R. C., Moore, M. J. K., Petters, M. D., Kreidenweis, S. M., Roberts, G. C., & Prather, K. A. (2009a). Effect of chemical mixing state on the hygroscopicity and cloud nucleation properties of calcium mineral dust particles. *Atmospheric Chemistry and Physics*, *9*, 3303–3316. https://doi.org/10.5194/acp-9-3303-2009

Sullivan, R. C., Moore, M. J. K., Petters, M. D., Kreidenweis, S. M., Roberts, G. C., & Prather, K. A. (2009b). Timescale for hygroscopic conversion of calcite mineral particles through heterogeneous reaction with nitric acid. *Physical Chemistry Chemical Physics*, *11*, 7826–7837. https://doi.org/10.1039/b904217b

Tan, F., Tong, S. R., Jing, B., Hou, S., Liu, Q., Li, K., et al. (2016). Heterogeneous reactions of NO_2 with $CaCO_3$–$(NH_4)_2SO_4$ mixtures at different relative humidities. *Atmospheric Chemistry and Physics*, *16*, 8081–8093. https://doi.org/10.5194/acp-16-8081-2016

Tang, I. N., & Fung, K. H. (1997). Hydration and Raman scattering studies of levitated microparticles: $Ba(NO_3)_2$, $Sr(NO_3)_2$, and $Ca(NO_3)_2$. *The Journal of Chemical Physics*, *106*, 1653–1660. https://doi.org/10.1063/1.473318

Tang, M. J., Cziczo, D. J., & Grassian, V. H. (2016). Interactions of water with mineral dust aerosol: Water adsorption, hygroscopicity, cloud condensation and ice nucleation. *Chemical Reviews*, *116*, 4205–4259. https://doi.org/10.1021/acs.chemrev.5b00529

Tang, M. J., Gu, W. J., Ma, Q. X., Li, Y. J., Zhong, C., Li, S., et al. (2019). Water adsorption and hygroscopic growth of six anemophilous pollen species: The effect of temperature. *Atmospheric Chemistry and Physics*, *19*, 2247–2258. https://doi.org/10.5194/acp-19-2247-2019

Tang, M. J., Huang, X., Lu, K. D., Ge, M. F., Li, Y. J., Cheng, P., et al. (2017). Heterogeneous reactions of mineral dust aerosol: Implications for tropospheric oxidation capacity. *Atmospheric Chemistry and Physics*, *17*, 11727–11777. https://doi.org/10.5194/acp-17-11727-2017

Tang, M. J., Whitehead, J., Davidson, N. M., Pope, F. D., Alfarra, M. R., McFiggans, G., & Kalberer, M. (2015). Cloud condensation nucleation activities of calcium carbonate and its atmospheric aging products. *Physical Chemistry Chemical Physics*, *17*, 32194–32203. https://doi.org/10.1039/c5cp03795f

Tang, M. J., Zhang, H. H., Gu, W. J., Gao, J., Jian, X., Shi, G. L., et al. (2019). Hygroscopic properties of saline mineral dust from different regions in China: Geographical variations, compositional dependence, and atmospheric implications. *Journal of Geophysical Research: Atmospheres*, *124*, 10844–10857. https://doi.org/10.1029/2019jd031128

Tang, Y., Carmichael, G. R., Kurata, G., Uno, I., Weber, R. J., Song, C. H., et al. (2004). Impacts of dust on regional tropospheric chemistry during the ACE-Asia experiment: A model study with observations. *Journal of Geophysical Research*, *109*, D19s21. https://doi.org/10.1029/2003jd003806

Textor, C., Schulz, M., Guibert, S., Kinne, S., Balkanski, Y., Bauer, S., et al. (2006). Analysis and quantification of the diversities of aerosol life cycles within AeroCom. *Atmospheric Chemistry and Physics*, *6*, 1777–1813. https://doi.org/10.5194/acp-6-1777-2006

Tobo, Y., Zhang, D., Matsuki, A., & Iwasaka, Y. (2010). Asian dust particles converted into aqueous droplets under remote marine atmospheric conditions. *Proceedings of the National Academy of Sciences of the United States of America*, *107*, 17905–17910. https://doi.org/10.1073/pnas.1008235107

Underwood, G. M., Li, P., Usher, C. R., & Grassian, V. H. (2000). Determining accurate kinetic parameters of potentially important heterogeneous atmospheric reactions on solid particle surfaces with a Knudsen cell reactor. *The Journal of Physical Chemistry A*, *104*, 819–829. https://doi.org/10.1021/jp9930292

Underwood, G. M., Miller, T. M., & Grassian, V. H. (1999). Transmission FT-IR and Knudsen cell study of the heterogeneous reactivity of gaseous nitrogen dioxide on mineral oxide particles. *The Journal of Physical Chemistry A*, *103*, 6184–6190. https://doi.org/10.1021/jp991586i

Uno, I., Eguchi, K., Yumimoto, K., Takemura, T., Shimizu, A., Uematsu, M., et al. (2009). Asian dust transported one full circuit around the globe. *Nature Geoscience*, *2*, 557–560. https://doi.org/10.1038/ngeo583

Usher, C. R., Michel, A. E., & Grassian, V. H. (2003). Reactions on mineral dust. *Chemical Reviews*, *103*, 4883–4939. https://doi.org/10.1021/cr020657y

Vlasenko, A., Sjogren, S., Weingartner, E., Stemmler, K., Gaggeler, H. W., & Ammann, M. (2006). Effect of humidity on nitric acid uptake to mineral dust aerosol particles. *Atmospheric Chemistry and Physics*, *6*, 2147–2160. https://doi.org/10.5194/acp-6-2147-2006

Wang, M. J., Zhu, T., Zhao, D. F., Rubach, F., Wahner, A., Kiendler-Scharr, A., & Mentel, T. F. (2018). Cloud condensation nuclei activity of $CaCO_3$ particles with oleic acid and malonic acid coatings. *Atmospheric Chemistry and Physics*, *18*, 7345–7359. https://doi.org/10.5194/acp-18-7345-2018

Zhang, Z., Shang, J., Zhu, T., Li, H., Zhao, D., Liu, Y., & Ye, C. (2012). Heterogeneous reaction of NO_2 on the surface of montmorillonite particles. *Journal of Environmental Sciences*, *24*, 1753–1758. https://doi.org/10.1016/s1001-0742(11)61014-0

Zhao, D. F., Buchholz, A., Mentel, T. F., Müller, K. P., Borchardt, J., Kiendler-Scharr, A., et al. (2010). Novel method of generation of $Ca(HCO_3)_2$ and $CaCO_3$ aerosols and first determination of hygroscopic and cloud condensation nuclei activation properties. *Atmospheric Chemistry and Physics*, *10*(17), 8601–8616. https://doi.org/10.5194/acp-10-8601-2010

Zhou, L., Wang, W., Hou, S., Tong, S., & Ge, M. (2015). Heterogeneous uptake of nitrogen dioxide on Chinese mineral dust. *Journal of Environmental Sciences*, *38*, 110–118. https://doi.org/10.1016/j.jes.2015.05.017